Supporting Information for

Structural heterogeneity of castor tissue lignins and their targeted conversion into sustainable aviation fuel precursors

Xu-Wei Wang,[a] Yu-Xin Zhang,[a] Xu Fu,[a] Qing-Hua Wang,[a] Qiang Wang,[a,*] Jun-Li Ren,[b] Ling-Ping Xiao,[a,c,*] and Run-Cang Sun[a]

[a] *Liaoning Key Lab of Lignocellulose Chemistry and BioMaterials, Liaoning Collaborative Innovation Center for Lignocellulosic Biorefinery, College of Light Industry and Chemical Engineering, Dalian Polytechnic University, Dalian 116034, China*

[b] *State Key Laboratory of Advanced Papermaking and Paper-based Materials, School of Light Industry and Engineering, South China University of Technology, Guangzhou 510640, China*

[c] *Instrumental Analysis Center, Dalian Polytechnic University, Dalian 116034, China*

*Correspondence authors.

E-mail addresses: wangqiang@dlpu.edu.cn (Q. Wang); lpxiao@dlpu.edu.cn (L.-P. Xiao).

Number of pages: 15

Number of tables: 5

Number of figures: 3

Quantification of Upgraded Cycloalkanes via the ECN Method

For the GC-FID quantification of the upgraded liquid cycloalkanes, n-dodecane was employed as the internal standard (IS). Since the targeted products are fully deoxygenated hydrocarbons, their effective carbon numbers (ECN) are equivalent to their actual carbon numbers. The mole ($n_{monomer}$) and weight ($W_{monomer}$) of each specific product were calculated using the following equations:

$$n_{IS} = \frac{W_{IS\ in\ sample}}{M_{WIS}}$$

$$n_{monomer} = n_{IS} \times \frac{A_{monomer\ in\ sample}}{A_{IS\ in\ sample}} \times \frac{ECN_{IS}}{ECN_{monomer}}$$

$$W_{monomer} = n_{monomer} \times M_{Wmonomer}$$

In these equations,

$W_{IS\ in\ sample}$ (mg): the weight of n-dodecane used as an internal standard in each analyzed sample;

M_{WIS} (mg/mmol): the molecular weight of n-dodecane (170 mg/mmol);

n_{IS} (mmol): the mole of n-dodecane in each analyzed sample;

$n_{monomer}$ (mmol): the mole of monomer in each analyzed sample;

$A_{monomer\ in\ sample}$: the peak area of monomer in the GC-FID chromatogram;

$A_{IS\ in\ sample}$: the peak area of n-dodecane in the GC-FID chromatogram;

ECN_{IS}: the effective carbon number of n-dodecane;

$ECN_{monomer}$: the effective carbon number of lignin monomer;

$W_{monomer}$ (mg): the weight of monomer in each analyzed sample;

FT-IR analysis

FT-IR spectra of lignin and lignin oil were recorded using a Perkin-Elmer spectrophotometer.

The spectra of powdered lignin supported by KBr pellets were recorded in the range of 400 to 4000 cm^{-1} with 32 scans averaged at 4.0 cm^{-1} resolution at room temperature.

GPC analysis

Gel permeation chromatography (GPC) analysis was conducted using a Waters HPLC system (Sunnyvale, CA) comprising an isocratic pump (Waters 1515), an autosampler (Waters 717), and a dual-wavelength UV detector (Waters 2487). Separation was achieved on an Agilent PLgel column (3 μm, 100 Å, 300 × 7.5 mm) with tetrahydrofuran (THF) as the mobile phase at a flow rate of 1.0 mL/min and a column temperature of 30 °C. Prior to analysis, lignin samples (2 mg) were dissolved in 1 mL of THF, filtered through a 0.45 μm PTFE membrane, and injected (20.0 μL) into the syringe. Detection was performed at 280 nm using the UV detector. Seven GPC polystyrene standards (124~26520 g/mol) purchased from Agilent (Agilent Technologies, Inc., Santa Clara, CA) were used for calibration. To enhance solubility and accuracy in GPC measurements, lignin was acetylated before analysis.[1-2] Briefly, 20 mg of lignin was reacted with 0.5 mL of pyridine and 0.5 mL acetic anhydride at 80 °C for 4 h. The product was precipitated in ice water (100 mL), centrifuged, and washed repeatedly to remove residual pyridine. The purified acetylated lignin was lyophilized and subsequently analyzed via GPC as described above.

GC and GC-MS analysis

GC and GC-MS analyses were carried out on a Shimadzu Model 2010 plus equipped with a HP-5 column (30 m × 0.25 mm × 0.25 μm) using a flame ionization detector (FID) and a Shimadzu GC-MS-QP 2010 pro equipped with a HP-5 MS (30 m × 0.25 mm × 0.25 μm) column, respectively. The injection temperature was 250 °C. The column temperature program was: 50 °C (3 min), 8 °C/min to 280 °C (5 min). The detection temperature was 200 °C for FID.[3] To ensure clarity and comparability, the monomer yield was calculated based on the mass of the initial EMAL substrate. The specific calculation formula is as follows:

$$\text{Monomer yield (wt\%)} = \frac{\text{Mass (total monomers)}}{\text{Mass (initial lignin)}} \times 100 \quad \text{(S4)}$$

where Mass (total monomers) is the quantified mass of the phenolic monomers in the liquid product, and Mass (initial lignin) is the exact initial weight of the EMAL loaded into the reactor.

TG Analysis

The thermal stability of the lignin samples was evaluated using a Q500 thermogravimetric analyzer (TA Instruments). In TG measurement, at a heating rate of 10 ^{o}C/min, approximately 10 mg of sample was placed in a small crucible under a nitrogen atmosphere at a temperature between 25 and 800 ^{o}C.[4]

Table S1 The chemical composition of Castor (*Ricinus communis* L.).

Sample	Ash (wt%)	lignin content (wt%)		cellulose content (wt%)	hemicellulose content (wt%)		
		KL	ASL	Glucose	Xylose	Arabinose	Galactose
Endocarp	2.54 ± 0.08	64.02 ± 1.15	2.02 ± 0.03	13.29 ± 0.02	10.27 ± 0.27	0.64 ± 0.05	1.10 ± 0.03
Epicarp	10.10 ± 0.02	13.88 ± 0.17	3.51 ± 0.08	37.70 ± 0.58	24.88 ± 0.47	0.72 ± 0.02	1.34 ± 0.03
Stalk	2.87 ± 0.12	18.69 ± 0.22	2.15 ± 0.16	45.78 ± 0.38	18.86 ± 0.43	0.64 ± 0.03	1.36 ± 0.01

Table S2 NMR data for the signal assignments for EMAL, LCC and lignin oils samples from various parts of castor in DMSO-d_6.

Label	δ_C/δ_H (ppm)	Assignment
D_β	53.3/3.46	C_β–H_β in β−5′ phenylcoumarane substructures (D)
B_β	53.5/3.06	C_β–H_β in β−β′ resinol substructures (B)
ArOMe	55.6/3.73	C–H in methoxyls
It_γ/A_γ	58.0-60.0/3.35–3.65	C_γ–H_γ in benzodioxane (I) and β-*O*-4′ substructures (A)
Ic_γ	58.4/3.35	C_γ–H_γ in cis-benzodioxane substructures (I)
E_γ	61.4/4.10	C_γ–H_γ in cinnamyl alcohol end-units (E)
D_γ	62.5/3.73	C_γ–H_γ in β−5′ phenylcoumaran substructures (D)
X_5	62.6/3.40–3.72	C_5–H_5 in β-D-xylopyranoside (X)
Est_γ	63.2/4.33	C_γ–H_γ in γ-ester lignin-carbohydrate complex structures
B_γ	71.0/3.82–4.18	C_γ–H_γ in β−β′ resinol substructures (B)
A_α	71.8/4.86	C_α–H_α in β-*O*-4′ substructures (A)
X_2	72.5/3.02	C_2–H_2 in β-D-xylopyranoside (X)
$X2_2$	73.2/4.49	C_2–H_2 in 2-*O*-acetyl-β-D-xylopyranoside (X)
X_3	73.7/3.22	C_3–H_3 in β-D-xylopyranoside (X)
$X3_3$	74.7/4.80	C_3–H_3 in 3-*O*-acetyl-β-D-xylopyranoside (X)
X_4	75.4/3.60	C_4–H_4 in β-D-xylopyranoside (X)
Ic_α	74.8/5.18	C_α–H_α in cis-benzodioxane substructures (I)
It_α	75.4/4.83	C_α–H_α in trans-benzodioxane substructures (I)
Ic_β	76.9/4.38	C_β–H_β in cis-benzodioxane substructures (I)
It_β	77.9/4.06	C_β–H_β in trans-benzodioxane substructures (I)
U_4	81.1/3.10	C_4–H_4 in 4-*O*-methyl-α-D-GlcUA (U)
$BE_{1\alpha}$	81.3/4.65	C_α–H_α in benzyl ether lignin-carbohydrate complex structures
$BE_{2\alpha}$	81.3/5.07	C_α–H_α in benzyl ether lignin-carbohydrate complex structures
$A_{\beta(G/H)}$	83.9/4.29	C_β–H_β in β-*O*-4′ substructures linked to G and H units (A)
B_α	84.8/4.65	C_α–H_α in β−β′ resinol substructures (B)
$A_{\beta(S)}$	85.9/4.12	C_β–H_β in β-*O*-4′ substructures linked to S units (A)
D_α	86.8/5.46	C_α–H_α in β−5′ phenylcoumaran substructures (D)
$\alpha X_{1(R)}$	92.2/4.88	C_1–H_1 in (1→4)-α-D-xylopyranoside (R)
U_1	97.2/5.18	C_1–H_1 in 4-*O*-methyl-α-D-GlcUA (U)

$\beta X_{1(R)}$	97.4/4.26	C_1–H_1 in (1→4)-β-D-xylopyranoside (R)
$PhGlc_1$	98.4/4.90	C_1–H_1 in phenyl glycoside linkages
R_1	98.8/5.12	C_1–H_1 in (1→2)-α-L-rhamnopyranoside (R)
$X23_1$	98.9/4.71	C_1–H_1 in 2,3-*O*-acetyl-β-D-xylopyranoside (X)
$X2_1$	99.4/4.52	C_1–H_1 in 2-*O*-acetyl-β-D-xylopyranoside (X)
$PhGlc_2$	100.6/4.65	C_2–H_2 in phenyl glycoside linkages
$PhGlc_3$	101 .5/4.79	C_3–H_3 in phenyl glycoside linkages
$X3_1$	101.6/4.32	C_1–H_1 in 3-*O*-acetyl-β-D-xylopyranoside (X)
X_1/Glc_1	103.2/4.20	C_1–H_1 in β-D-xylopyranoside/β-D-glucopyranoside
$S_{2/6}$	103.8/6.71	$C_{2/6}$–$H_{2/6}$ in etherified syringyl units (S)
$S'_{2/6}$	106.2/7.23–7.07	$C_{2/6}$–$H_{2/6}$ in oxidized (C_α=O) syringyl units (S′)
G_2	110.9/6.98	C_2–H_2 in guaiacyl units (G)
G'_2	111.4/7.51	C_2–H_2 in oxidized (C_α=O) guaiacyl units (G′)
C_2, C_5, C_6	112.0–120.0/7.20	C_2–H_2, C_5–H_5, C_6–H_6, in etherified catechyl units (C)
G_5	114.9/6.77	C_2–H_2 in guaiacyl units (G)
$H_{3/5}$	114.9/6.77	$C_{3/5}$–$H_{3/5}$ in *p*-hydroxyphenyl units (H)
FA_8	114.8/6.49	C_8/H_8 in ferulates (FA)
$PB_{3/5}$	114.9/6.77	$C_{3/5}$–$H_{3/5}$ in *p*-hydroxybenzoate substructures (PB)
$pCA_{3/5}$	115.5/6.77	C_3/H_3 and C_5/H_5 in *p*-coumarates (*p*CA)
G_6	119.0/6.80	C_6-H_6 in guaiacyl units (G)
J_β	126.1/6.76	C_β–H_β in cinnamaldehyde end groups (J)
$H_{2/6}$	127.9/7.19	$C_{2/6}$–$H_{2/6}$ in p-hydroxyphenyl units (H)
E_α	128.4/6.44	C_α–H_α in cinnamyl alcohol end-units (E)
E_β	128.7/6.20	C_β–H_β in cinnamyl alcohol end-units (E)
$pCA_{2/6}$	129.9/7.45	C_2/H_2 and C_6/H_6 in *p*-coumarates (*p*CA)
$PB_{2/6}$	131.2/7.67	$C_{2/6}$–$H_{2/6}$ in p-hydroxybenzoate substructures (PB)
pCA_7/FA 7	144.7/7.58	C_7/H_7 in p-coumarates (*p*CA) and ferulates (FA)
J_α	153.5/7.60	C_α–H_α in cinnamaldehyde end groups (J)
$C3_\alpha$	38.2/2.61	C_α–H_α in compound C3
$C3_\beta$	24.1/1.64	C_β–H_β in compound C3
$C3_\gamma$	13.7/0.94	C_γ–H_γ in compound C3
$C4_\alpha$	131.5/6.21	C_α–H_α in compound C4
$C4_\beta$	121.7/5.94	C_β–H_β in compound C4
$C4_\gamma$	18.1/1.80	C_γ–H_γ in compound C4
$G/S2_\alpha$	28.3/2.48	C_α–H_α in compounds G2 and S2

G/S2$_{\beta}$	16.4/1.14	C_{β}–H_{β} in compounds G2 and S2
G/S3$_{\alpha}$	37.5/2.43	C_{α}–H_{α} in compounds G3 and S3
G/S3$_{\beta}$	24.9/1.55	C_{β}–H_{β} in compounds G3 and S3
G/S3$_{\gamma}$	13.9/0.87	C_{γ}–H_{γ} in compounds G3 and S3
G/S4$_{\alpha}$	31.1/2.51	C_{α}–H_{α} in compounds G4 and S4
G/S4$_{\beta}$	34.4/1.70	C_{β}–H_{β} in compounds G4 and S4
G/S4$_{\gamma}$	60.6/3.43	C_{γ}–H_{γ} in compounds G4 and S4
H1$_{\alpha}$	19.7/2.19	C_{α}–H_{α} in compounds H1
H2$_{\alpha}$	29.3/2.71	C_{α}–H_{α} in compounds H2
H2$_{\beta}$	35.5/1.52	C_{β}–H_{β} in compounds H2

Table S3 The weight-average (M_w) and number-average (M_n) molecular weights and the polydispersity (M_w/M_n = PDI) of EMAL, lignin oil, LCC and HDO products.

Sample	M_w	M_n	PDI
Endocarp EMAL	3485	1660	2.10
Epicarp EMAL	9390	1895	4.96
Stalk EMAL	10295	2210	4.66
Endocarp lignin oil	230	83	2.77
Epicarp lignin oil	465	154	3.02
Stalk lignin oil	395	149	2.65
Endocarp LCC	1450	890	1.63
Epicarp LCC	2045	1025	2.00
Stalk LCC	3170	1020	3.11
Endocarp	155	145	1.07
Epicarp	150	140	1.11
Stalk	150	140	1.11

Table S4 The hydroxyl group contents of various EMAL samples (millimoles per gram).

EMAL Samples	Aliphatic OH	Phenolic					*p*CA-OH	Catechol OH	Carboxylic Group	Total Phenolic OH
		Cond. G [a]	Non. Cond. G [a]	Cond. S [a]	Non. Cond. S [a]	Non. Cond. H [a]				
Endocarp	3.43	– [b]	–	–	–	–	–	3.27	0.10	3.27
Epicarp	4.37	0.06	0.31	0.03	0.09	0.60	0.31	–	0.07	1.40
Stalk	4.50	0.17	0.49	0.05	0.14	0.03	–	–	0.06	0.88

[a] "Cond. and Non. Cond." represents condensed phenolic units and non-condensed phenolic units, respectively.

[b] Signifies not detected.

Table S5 Typical chemical shifts and integration regions for EMAL samples from various parts of castor in the ^{31}P NMR spectra.

Structure	δ (ppm)
Aliphatic OH	145.40–150.00
Condensed guaiacyl OH	141.42–142.17
Noncondensed guaiacyl OH	138.79–140.17
Condensed syringyl OH	143.20–144.50
Noncondensed syringyl OH	142.17–143.20
p-coumarate (*p*CA) OH	136.70–137.80
Noncondensed *p*-hydroxyphenyl OH	137.10-138.40
Catechol OH	138.0–140.0
Carboxylic group	134.2–135.5

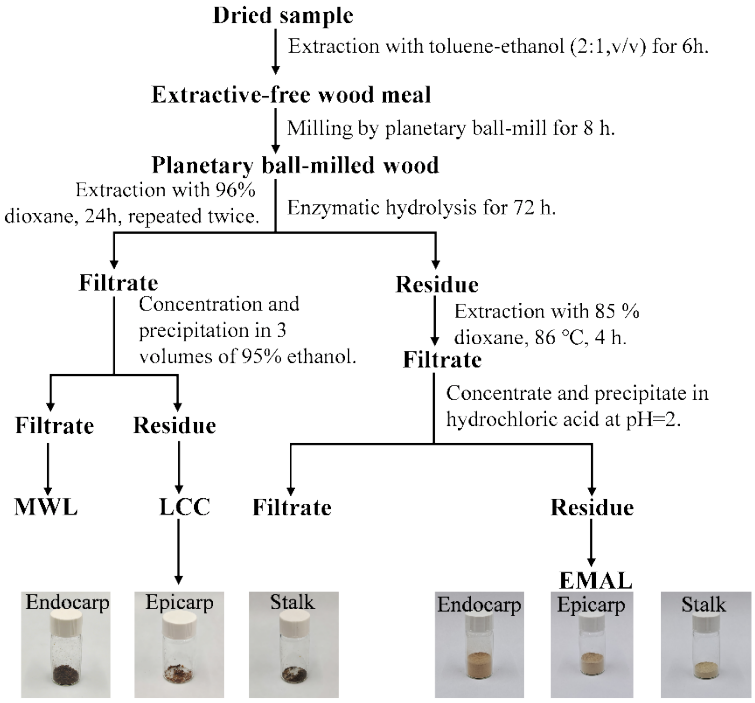

Fig. S1 Extraction process of EMAL and LCC fractions.

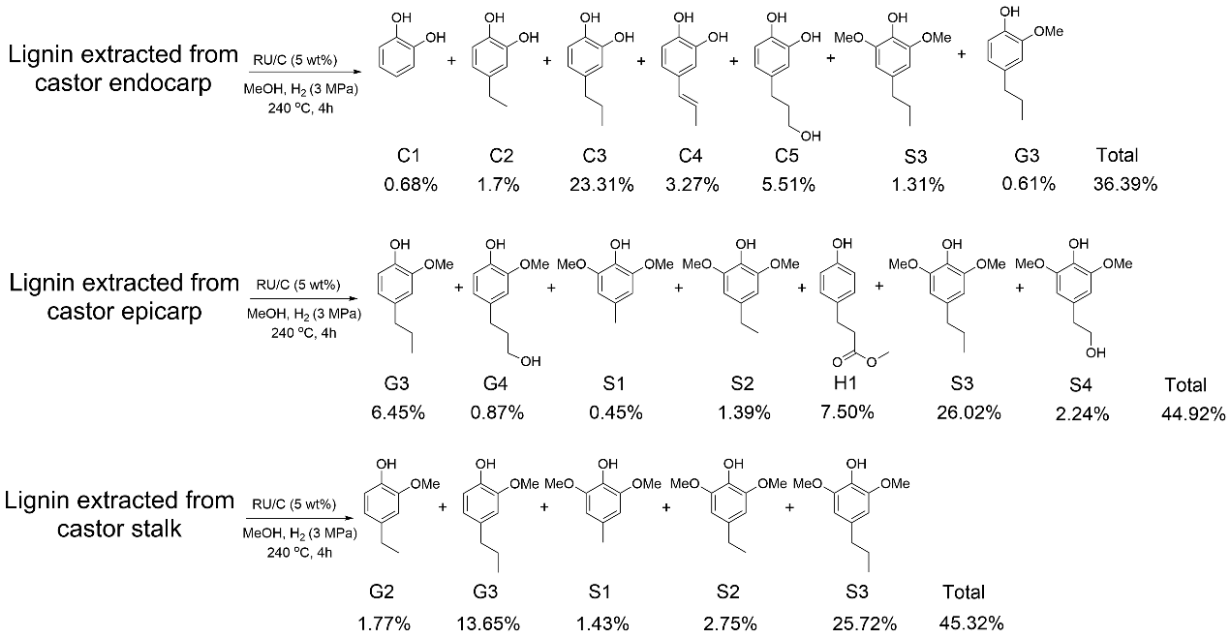

Fig. S2 Monomer yields from the hydrogenolysis of EMAL samples from three different parts of Castor.

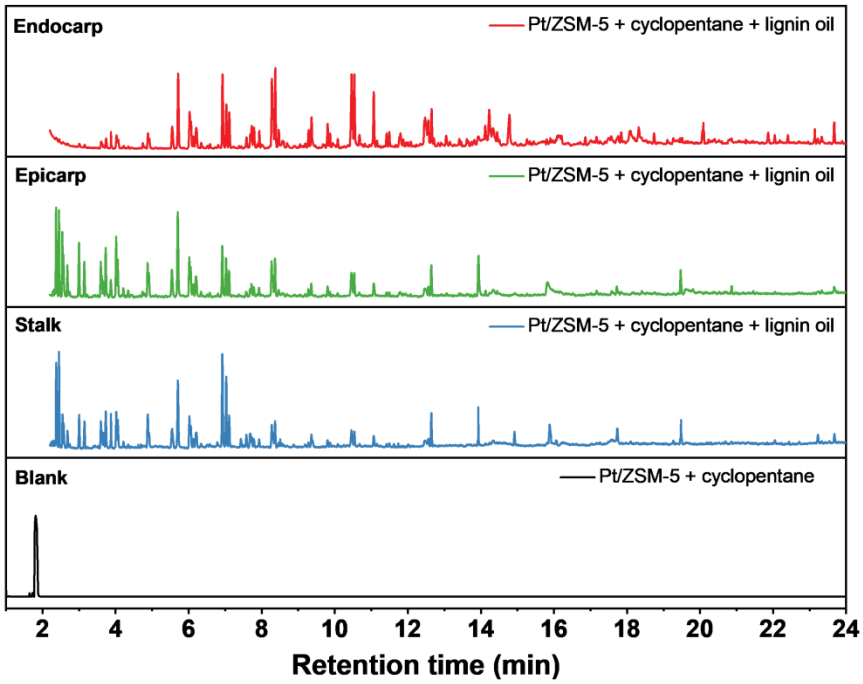

Fig. S3 GC chromatograms of the reaction mixtures from the HDO of castor-derived lignin oil (endocarp, epicarp, and stalk) and the blank experiment (Pt/ZSM-5 + cyclopentane) under identical reaction conditions.

References

1 D. J. McClelland, A. H. Motagamwala, Y. Li, M. R. Rover, A. M. Wittrig, C. Wu, J. S. Buchanan, R. C. Brown, J. Ralph, J. A. Dumesic and G. W. Huber, *Green Chem.*, 2017, **19**, 1378-1389. DOI: 10.1039/c6gc03515a.

2 M. M. Abu-Omar, K. Barta, G. T. Beckham, J. S. Luterbacher, J. Ralph, R. Rinaldi, Y. Román-Leshkov, J. S. M. Samec, B. F. Sels and F. Wang, *Energy Environ. Sci.*, 2020, **14**, 262-292. DOI: 10.1039/d0ee02870c.

3 Y. Liao, S.-F. Koelewijn, G. Van den Bossche, J. Van Aelst, S. Van den Bosch, T. Renders, K. Navare, T. Nicolaï, K. Van Aelst, M. Maesen, H. Matsushima, J. M. Thevelein, K. Van Acker, B. Lagrain, D. Verboekend and B. F. Sels, *Science*, 2020, **367**, 1385-1390. DOI: 10.1126/science.aau1567.

4 X. Huang, H. Yin, H. Zhang, N. Mei and L. Mu, *Energy*, 2022, **259**, 125062. DOI: 10.1016/j.energy.2022.125062.